

APPLICATION OF COMPLETE COMPLEMENTARY SEQUENCE IN ORTHOGONAL MIMO SAR SYSTEM

S. F. Li, J. Chen, L. Q. Zhang, and Y. Q. Zhou

201 Lab, School of Electronic and Information Engineering
Beihang University
Beijing 100191, China

Abstract—The Complete Complementary Sequence (CC-S) consists of several complementary orthogonal sequences and has optimal sidelobe level performance, which is satisfied with the requirement of the orthogonal Multiple Input Multiple Output (MIMO) radar signals. Aimed at the difficulty of high sidelobe level in Synthetic Aperture Radar (SAR) imaging processing in range dimension, an approach of depressing sidelobe level based on CC-S in MIMO SAR system was proposed. The transmitter model for orthogonal MIMO SAR system using CC-S and the corresponding matched filter (MF) were established in this paper. In addition, the MIMO SAR imaging results were simulated. The simulation results demonstrate that the performance of CC-S employed in orthogonal MIMO radar system is much better than that with traditional Linear Frequency Modulation (LFM) signal, by which the feasibility and validity of CC-S applied in orthogonal MIMO SAR system are justified.

1. INTRODUCTION

MIMO radar is a new concept proposed in recent years [1–7]. The waveforms requirements differ between MIMO and multi-channel antenna system. In MIMO radar, there are several transmitters which are transmitting multiple orthogonal or non-coherent waveforms and several receivers which are receiving the echoes reflected by the targets, while the traditional multi-channel antenna system transmits multiple coherent waveforms in the transmitter. MIMO radar systems are mainly divided into two important categories. In the first category, different transmit and receive antenna elements are close to each other, so that the system can exploit the waveform diversity offered

Corresponding author: S. F. Li (shufeng_2004@163.com).

by orthogonal signals to achieve coherent processing, increase the degree of freedom and improve the parameter estimation performance. We refer to the system as orthogonal MIMO radar [8–12]. In the second category, transmitter and receiver elements are far from each other relative to the transmitted wavelength. In this case, the MIMO radar system utilizes the widely separated antennas to obtain non-coherent processing to obtain target detection and estimation of various parameters [13–16]. The system in this category is mostly known as statistic MIMO radar [17–19]. This paper focuses on the MIMO radar based on CC-S which is categorized as the orthogonal MIMO radar.

Orthogonal MIMO radar transmits orthogonal signal set, and the receivers extract the corresponding echo by matched filter. The design of transmitted signal impacts on the orthogonal MIMO radar system performance directly. In order to constrict interference and enhance the target resolution, the signal employed in orthogonal MIMO radar should have good auto- and cross- correlations, even have ideal correlation property (the sidelobes of aperiod auto- and cross- correlations are zero). Orthogonal MIMO radar mainly utilizes orthogonal phase coding and orthogonal frequency coding in preceding literature [20–23]. The sidelobe levels of above two codes will deteriorate the imaging result, while CC-S utilizes the complementary pair to cancel the sidelobe and to improve the imaging quality. The CC-S opens a new direction for the signal design of orthogonal MIMO radar.

The advantage of SAR techniques is that they are independent of the weather condition, day and night, which plays critical roles in imaging sensors. With the development of the MIMO radar, drawing the concept of MIMO into SAR domain becomes an interest topic for MIMO radar [24–27]. Through a deterministic array and spatial parallel sampling procedure, the problem of motion compensation was solved in [24]. The correlation among distribution of transmitter/receiver antenna, imaging performance and spatial spectral domain filling is analyzed in [25]. The above references mainly refer to the ground-based radar. This paper mainly presents the research of airborne MIMO SAR. The orthogonal signals are required in MIMO SAR system, so exploring the available orthogonal signals determines the practical application of MIMO SAR. The MIMO SAR imaging algorithm based on CC-S is analyzed in this paper. Owing to the zero sidelobe level correlation function of CC-S, the system can obtain the high peak sidelobe level ratio (PSLR) and integration sidelobe level ratio (ISLR) without depressing sidelobe level, while traditional SAR system acquire the high PSLR through applying

window function, thus result in the broadening of mainlobe and the decrease of the resolution; the MIMO SAR system based on CC-S guarantee the high PSLR and high resolution at the same time.

The outline of this paper is arranged as follows: Section 2 presents the orthogonal signal model of the MIMO SAR and the concept of CC-S. This is done in order to introduce ideas and notation to be used later in imaging algorithm based on CC-S. The receiver design and matched filter based on CC-S are proposed in Section 3. In Section 4, the imaging results is briefly discussed and displayed via the results of simulation. A summary including conclusions is presented in Section 5.

2. SIGNAL MODEL OF AIRBORNE MIMO SAR

The model of MIMO SAR is shown in Fig. 1, where we see that the platform is supposed to fly along the x -axis at height h and velocity v during the constant altitude acquisition time, the M transmitters and N receivers of the linear array are equally spaced along the x -axis, where d and l is the inter-element spacing of transmitters and receivers respectively, θ is the squint angle of the first transmitter, γ is the pitch angle, the location of the target is (x_T, y_T) . When $t = 0$, the instant slant range between the swath center $\mathbf{0}$ and antenna phase center is $R_m(t)$ for m -th transmitter and $R_n(t)$ for the n -th receiver.

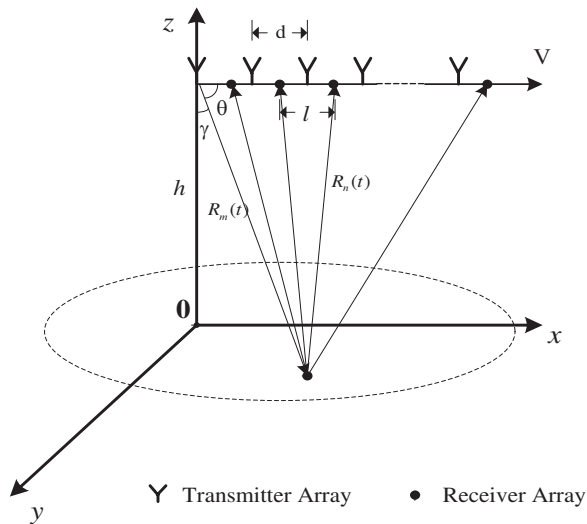


Figure 1. Model of the antenna array.

At time t , $R_m(t)$ and $R_n(t)$ are expressed as follows:

$$\begin{cases} R_m(t) = \sqrt{(vt + md - x_T)^2 + y_T^2 + h^2} \\ R_n(t) = \sqrt{(vt + nl - x_T)^2 + y_T^2 + h^2} \end{cases} \quad (1)$$

Using a Taylor series expansion, (1) can be written as:

$$\begin{cases} R_m(t) \approx R_m + \frac{md - x_T}{R_m} vt + \frac{1}{2} \left(\frac{1}{R_m} - \frac{(md - x_T)^2}{R_m^3} \right) v^2 t^2 \\ R_n(t) \approx R_n + \frac{nl - x_T}{R_n} vt + \frac{1}{2} \left(\frac{1}{R_n} - \frac{(nl - x_T)^2}{R_n^3} \right) v^2 t^2 \end{cases} \quad (2)$$

where $|t| \leq \frac{T_s}{2}$, T_s denotes the synthetic aperture time, in expression (2), $R_m = \sqrt{(md - x_T)^2 + y_T^2 + h^2} \approx R + \frac{m^2 d^2 - 2mdx_T}{2R}$, $R_n = \sqrt{(nl - x_T)^2 + y_T^2 + h^2} \approx R + \frac{n^2 l^2 - 2nlx_T}{2R}$. Where $R = \sqrt{x_T^2 + y_T^2 + h^2}$, under the condition of far field, the length of antenna can be omitted with the distance between antenna and the target, the (2) can be approximated as:

$$\begin{cases} R_m(t) \approx R + \frac{m^2 d^2 - 2mdx_T}{2R} + \frac{md - x_T}{R} vt + \frac{1}{2} \left(\frac{1}{R} - \frac{(md - x_T)^2}{R^3} \right) v^2 t^2 \\ R_n(t) \approx R + \frac{n^2 l^2 - 2nlx_T}{2R} + \frac{nl - x_T}{R} vt + \frac{1}{2} \left(\frac{1}{R} - \frac{(nl - x_T)^2}{R^3} \right) v^2 t^2 \end{cases} \quad (3)$$

where $R = h/(\cos \gamma \cdot \cos \theta)$ is the distance between target and the first transmitter, the phase delay during the flying is:

$$\phi_{mn}(t) = -\frac{2\pi}{\lambda} [R_m(t) + R_n(t)] \quad (4)$$

The Doppler frequency is:

$$\begin{aligned} f_{d_{mn}}(t) &= \frac{1}{2\pi} \frac{d\phi_{mn}(t)}{dt} = - \left(\frac{md - x_T}{\lambda R} + \frac{nl - x_T}{\lambda R} \right) v \\ &\quad - \left(\frac{2}{\lambda R} - \frac{(md - x_T)^2 + (nl - x_T)^2}{\lambda R^3} \right) v^2 t = f_{d_{mn}} + f_{r_{mn}} \cdot t \end{aligned} \quad (5)$$

where the Doppler centroid frequency:

$$f_{d_{mn}} = f_{d_{mn}}(t) \Big|_{t=0} = - \left(\frac{md - x_T}{\lambda R} + \frac{nl - x_T}{\lambda R} \right) v \quad (6)$$

The Doppler modulation frequency:

$$f_{r_{mn}} = f'_{d_{mn}}(t) \Big|_{t=0} = - \left(\frac{2}{\lambda R} - \frac{(md - x_T)^2 + (nl - x_T)^2}{\lambda R^3} \right) v^2 \quad (7)$$

The next will introduce the model of transmitted signals. We assume that the M transmitting signal is in the same frequency, meeting the orthogonality, the m -th signal is $s_m(\tau)$, define the correlation function by:

$$\int s_m(\tau)s_n^*(\tau)d\tau = \begin{cases} 1, & m = n \\ c_{m,n}, & m \neq n \end{cases} \quad (8)$$

where τ is the fast time, $c_{m,n}$ denotes the cross-correlation value of different transmitted signals, if the condition $c_{m,n} \equiv 0(m \neq n)$ is satisfied, the transmitted signals are orthogonal. There are no complete orthogonal signal in the single code field, while the CC-S meet the condition of orthogonality, and need the multiple channels in the practical application. Thus we employ the CC-S in the MIMO SAR system for exploiting the above property to analyze the MIMO SAR imaging based on CC-S. We will present the concept of CC-S in the next section.

Definition 1 Supposing that $\{A_m, B_m\}$ consists of M pairs of complementary sequence, the length of A_m and B_m is L . $\{A_m, B_m\}$ is called CC-S if both the following correlation function conditions are satisfied:

i) For every $i = 1, 2, \dots, M$, it holds that

$$R_{A_i A_i}(\tau) + R_{B_i B_i}(\tau) = \begin{cases} 2L & \tau = 0 \\ 0 & \tau = \pm 1, \pm 2, \dots, \pm(L-1) \end{cases} \quad (9)$$

ii) For every $1 \leq m, n \leq M, m \neq n$, it holds that

$$R_{A_m A_n}(\tau) + R_{B_m B_n}(\tau) = 0 \quad \tau = 0, \pm 1, \pm 2, \dots, \pm(L-1) \quad (10)$$

where $R_{A_m A_n}(\tau)$ denotes the aperiod correlation function between A_m and A_n , and $R_{B_m B_n}(\tau)$ denotes the aperiod correlation function between B_m and B_n . The (9) describes the auto-correlation function (ACF) and (10) shows the cross-correlation function (CCF) of the CC-S respectively. The orthogonal MIMO radar transmitter model based on CC-S is shown in Fig. 2.

From Fig. 2, we can see that A_m and $B_m(0 \leq m \leq M)$ constitute a complementary pair, T denotes the delay time, and f_c is the carrier frequency. The definition of M pairs of complementary sequence $\{A_m, B_m\}$ is given as:

$$\begin{cases} A_m = (a_m^0, a_m^1, \dots, a_m^{L-1}) \\ B_m = (b_m^0, b_m^1, \dots, b_m^{L-1}) \end{cases} \quad (11)$$

where $\{(A_0, B_0), (A_1, B_1), \dots, (A_M, B_M)\}$ meet the complete orthogonality and make up a family of CC-S. A_m and B_m are transmitted in

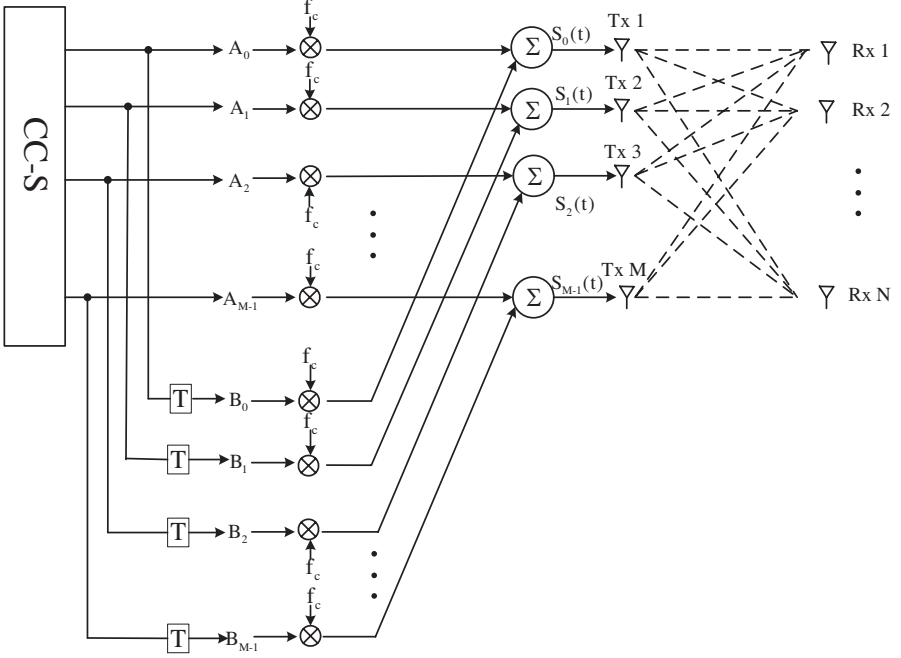


Figure 2. Transmitter model based on CC-S.

m -th antenna by turns, the m -th transmitted signal $s_m(\tau)$ is:

$$\begin{aligned}
 s_m(\tau) &= \sum_{l=0}^{L-1} \left[a_m^l \cdot \text{rect}_{\tau_p}(\tau - l \cdot T) + b_m^l \cdot \text{rect}_{\tau_p}(\tau - T - l \cdot T_c) \right] \cdot e^{j2\pi f_c \tau} \\
 &= [s_{A_m}(\tau) + s_{B_m}(\tau - T)] \cdot e^{j2\pi f_c \tau}
 \end{aligned} \quad (12)$$

where T also denotes the pulse repetition time, T_c is the subpulse time, $\tau_p = L \cdot T_c$ is the pulse duration time, and $\text{rect}_{\tau_p}(t)$ denotes the rectangle window function:

$$\text{rect}_{\tau_p}(t) = \begin{cases} 1 & 0 \leq t \leq \tau_p \\ 0 & \text{else} \end{cases} \quad (13)$$

3. MIMO SAR IMAGING ALGORITHM BASED ON CC-S

The system employs the CC-S in MIMO SAR. Due to the complete orthogonality of CC-S, the range dimension and azimuth dimension can be processed independently. The range dimension compression is described as following:

3.1. The Compression of Range Dimension

The echo signal $y_n(\tau, t)$ arrived at the n -th receiver is:

$$y_n(\tau, t) = \sum_{m=0}^{M-1} A_r \left[s_{A_m} \left(\tau - \frac{R_m(t) + R_n(t)}{c} \right) + s_{B_m} \left(\tau - \frac{R_m(t) + R_n(t)}{c} - T \right) \right] \cdot w_a(t - t_c) \cdot e^{j2\pi f_c \left(\tau - \frac{R_m(t) + R_n(t)}{c} \right)} = y_{n,A_m}(\tau) + y_{n,B_m}(\tau - T) \quad (14)$$

where A_r denotes the complex amplitude of the received signal, $w_a(t)$ is the azimuth envelope, and t_c is beam center offset time. The structure of receiver is shown in Fig. 3. There are M sub-channels in the receiver, and the sub-channel extracts the corresponding echo data by matched filter.

Aimed at the dual code property of CC-S, the sub-receiver in Fig. 3 is described in Fig. 4.

We define:

$$\tilde{R}(m, n) = \frac{m^2 d^2 + n^2 l^2 - 2x_T(md + nl)}{2R} \quad (15)$$

The echo arrived at the m -th sub-receiver of the n -th antenna can

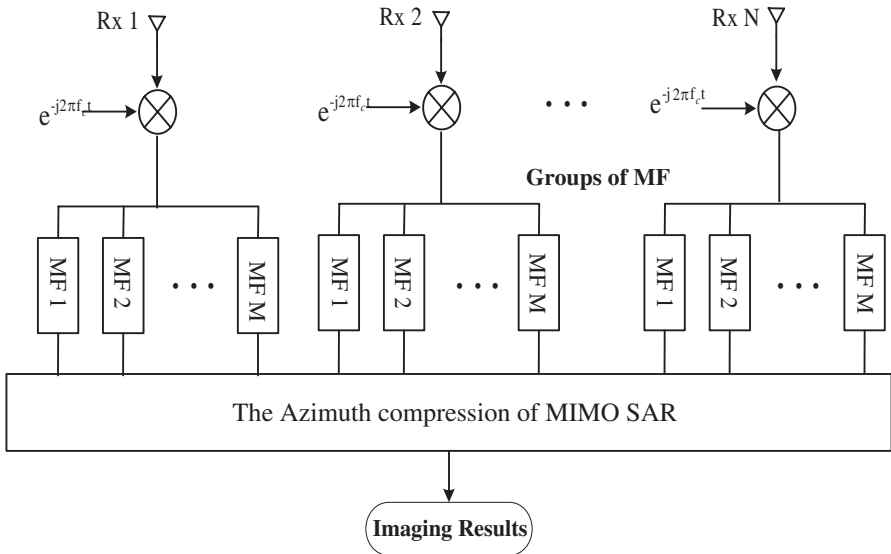


Figure 3. Structure of MIMO radar receiver.

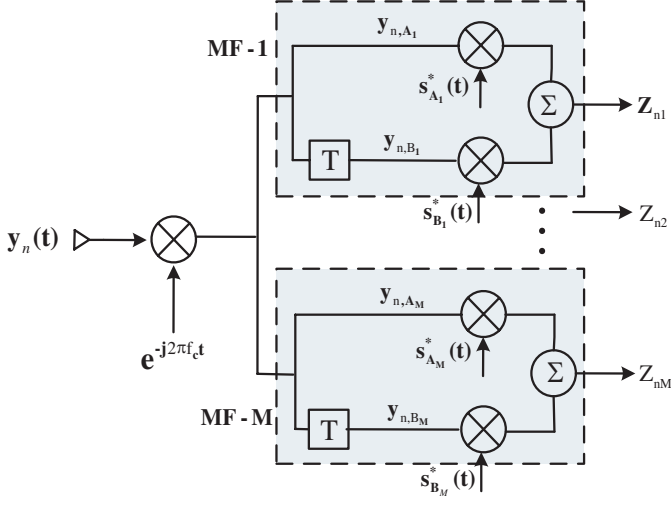


Figure 4. Sub-receiver matched filter based on CC-S.

be stated as:

$$\begin{aligned}
 y_{nm}(\tau, t) &= \int_t^{t+T} y_n(\tau, t) \cdot s_m^*(\tau) d\tau \\
 &= A_r w_a(t - t_c) \left[\int_t^{t+T} \sum_{i=1}^M e^{-j2\pi f_c \frac{R_i(t)+R_n(t)}{c}} s_{A_i}(\tau) \cdot s_{A_m}^*(\tau) d\tau \right. \\
 &\quad \left. + \int_t^{t+T} \sum_{i=1}^M e^{-j2\pi f_c \frac{R_i(t)+R_n(t)}{c}} s_{B_i}(\tau) \cdot s_{B_m}^*(\tau) d\tau \right] \\
 &= A_r \cdot 2L \cdot \delta \left(\tau - \frac{R_m(t) + R_n(t)}{c} \right) \\
 &\quad \cdot w_a(t - t_c) \cdot e^{-j\frac{2\pi}{\lambda} \left\{ [2R + \tilde{R}(m, n)] - \frac{\lambda}{2} f_{d_{mn}} \cdot t - \frac{\lambda}{4} f_{r_{mn}} \cdot t^2 \right\}} \\
 &\quad + A_r \cdot w_a(t - t_c) \cdot \left[\int_t^{t+T} \sum_{\substack{i=1 \\ i \neq m}}^M [s_{A_i}(\tau) \cdot s_{A_m}^*(\tau) + s_{B_i}(\tau) s_{B_m}^*(\tau)] \right. \\
 &\quad \left. e^{-j\frac{2\pi}{\lambda} \left\{ \left[2R + \frac{i^2 d^2 + n^2 l^2 - 2x_T(id+nl)}{2R} \right] + \left[\frac{id+nl-2x_T}{R} \right] vt \right\}} \right. \\
 &\quad \left. + \left[\frac{1}{R} - \frac{(id-x_T)^2 + (nl-x_T)^2}{2R^3} \right] v^2 t^2 \right\} d\tau \right] \quad (16)
 \end{aligned}$$

The first part of (16) is the contribution of auto-correlation and the second part denotes the contribution of cross-correlation. The complementary property of $\{A_m, B_m\}$ will be used to cancel the sidelobe, thus the second part becomes zero. The (16) can be summarized as:

$$y_{nm}(\tau, t) = A_r \cdot 2L \cdot \delta \left(\tau - \frac{R_m(t) + R_n(t)}{c} \right) \cdot w_a(t - t_c) \cdot e^{-j\frac{2\pi}{\lambda} \{ [2R + \tilde{R}(m, n)] - \frac{\lambda}{2} f_{d_{mn}} \cdot t - \frac{\lambda}{4} f_{r_{mn}} \cdot t^2 \}} \quad (17)$$

when $m = n = 0$, (17) is degenerated as the traditional monostatic SAR system. For our purpose, we simplify the const value as G in above expression, so (17) becomes:

$$y_{nm}(\tau, t) = G \cdot \delta \left(\tau - \frac{R_m(t) + R_n(t)}{c} \right) \cdot w_a(t - t_c) \cdot e^{[j(\pi f_{d_{mn}} t + \frac{1}{2} \pi f_{r_{mn}} t^2)]} \quad (18)$$

How to extract the scattering function of the target from $\{y_{nm}\}_{m, n=0}^{M-1, N-1}$ is a crucial technique in MIMO SAR imaging domain.

3.2. The Compression of Azimuth Dimension

We can convert the echo in the range time domain into Range-Doppler domain by Fast Fourier Transform (FFT). By using principle of stationary phase (POSP), the time-frequency expression of azimuth time domain is:

$$f_t = \frac{1}{2} (f_{d_{mn}} + f_{r_{mn}} \cdot t) \quad (19)$$

By substituting $t = (2f_t - f_{d_{mn}}) / f_{r_{mn}}$ into (17), the data after the azimuth FFT can be expressed as:

$$\begin{aligned} Y_{nm}(\tau, f_t) &= FFT_t \{y_{nm}(\tau, t)\} \\ &= G \cdot \delta \left(\tau - \frac{R_m(f_t) + R_n(f_t)}{c} \right) \cdot W_a(f_t - f_{t_c}) \\ &\quad \cdot e^{-j\frac{2\pi}{\lambda} \tilde{R}(m, n)} \cdot e^{-j\pi \frac{f_{d_{mn}}^2}{2f_{r_{mn}}}} \cdot e^{j\pi \frac{2f_t^2}{f_{r_{mn}}}} \end{aligned} \quad (20)$$

The azimuth beam pattern, $w_a(t - t_c)$, is now transformed into $W_a(f_t - f_{t_c})$, with its shape preserved. Combining (19) and (3), the distance function becomes:

$$R_m(f_t) + R_n(f_t) = 2R + \tilde{R}(m, n) + f_{d_{mn}} \frac{2f_t - f_{d_{mn}}}{f_{r_{mn}}} + \frac{1}{2} f_{r_{mn}} \cdot \left(\frac{2f_t - f_{d_{mn}}}{f_{r_{mn}}} \right)^2 \quad (21)$$

The amount to correct is given by the last two terms in (21):

$$\Delta R(f_t) = f_{d_{mn}} \cdot \frac{2f_t - f_{d_{mn}}}{f_{r_{mn}}} + \frac{1}{2} f_{r_{mn}} \cdot \left(\frac{2f_t - f_{d_{mn}}}{f_{r_{mn}}} \right)^2 \quad (22)$$

The echo after range cell migration correction (RCMC) becomes:

$$Y_{nm}(\tau, f_t) = G \cdot \delta \left(\tau - \frac{2R + \tilde{R}(m, n)}{c} \right) \cdot W_a(f_t - f_{t_c}) \cdot e^{-j\frac{2\pi}{\lambda} \tilde{R}(m, n)} \cdot e^{-j\pi \frac{f_{d_{mn}}^2}{2f_{r_{mn}}}} \cdot e^{j\pi \frac{2f_t^2}{f_{r_{mn}}}} \quad (23)$$

We can focus the azimuth data through the matched filter. According to the characteristic of MIMO SAR system based on CC-S, there are two sorts of solutions to focus the azimuth data:

1. Every channel uses Doppler parameter differently to compress the data in azimuth dimension, thus we can get $M \cdot N$ images which can be utilized for interferometry processing, clutter canceling and ground moving target indication (GMTI) and so on.
2. We can sum the data after range pulse compression firstly, and then use the identical Doppler parameter to focus the data in azimuth dimension. The imaging quality using the first solution is much better than the second solution due to the different Doppler parameter. The two solutions are closely in the imaging performance under the condition that the squint angle is small. The second solution is applied in real-time processing for the sake of the low computation. We employ the first solution in this paper.

The azimuth reference function is expressed by:

$$H_{nm}(f_t) = e^{-j\pi \frac{2f_t^2}{f_{r_{mn}}}} \quad (24)$$

The data after azimuth pulse compression is:

$$\begin{aligned} y_{nm}(\tau, t) &= IFFT_t \{ Y_{nm}(\tau, f_t) H_{nm}(f_t) \} \\ &= G \cdot \delta \left(\tau - \frac{2R + \tilde{R}(m, n)}{c} \right) \cdot w_a(t) e^{-j\frac{2\pi}{\lambda} \tilde{R}(m, n)} \cdot e^{-j\pi \frac{f_{d_{mn}}^2}{2f_{r_{mn}}}} \cdot e^{j2\pi f_{t_c} t} \end{aligned} \quad (25)$$

4. SIMULATION EXPERIMENTS

To validate the effectiveness of the proposed MIMO SAR imaging algorithm based on CC-S, we carry out the following experiment. We simulated the 2-Input 2-Output system. The CC-S $\{(A_0, B_0), (A_1, B_1)\}$ constructed in [28] is applied in MIMO SAR system. A_0 and B_0 are

transmitted in transmitter 1 by turns, while A_1 and B_1 are transmitted in transmitter 2 by turns. In the antenna geometry defined as Fig. 1, we locate nine point targets which have the same scattering coefficient and the geometry parameters: $d = 0.5\lambda$, $l = 0.5\lambda$, $\gamma = 24^\circ$, for simplification of the MIMO SAR system, we set $\theta = 90^\circ$. The key simulation parameters of the MIMO SAR system are listed in Table 1.

Table 1. MIMO SAR simulation parameters.

Parameter	Value
Wavelength	0.018 m
Sub-pulse time	0.025 μ s
Signal bandwidth	40 MHz
Sampling rates	50 MHz
Azimuth antenna length	2 m
PRF	220 Hz
Height	5 km
Velocity	120 m/s
Synthetic Aperture Time	0.84 s
Slant Range	11.225 km
Azimuth antenna beamwidth	0.516 $^\circ$

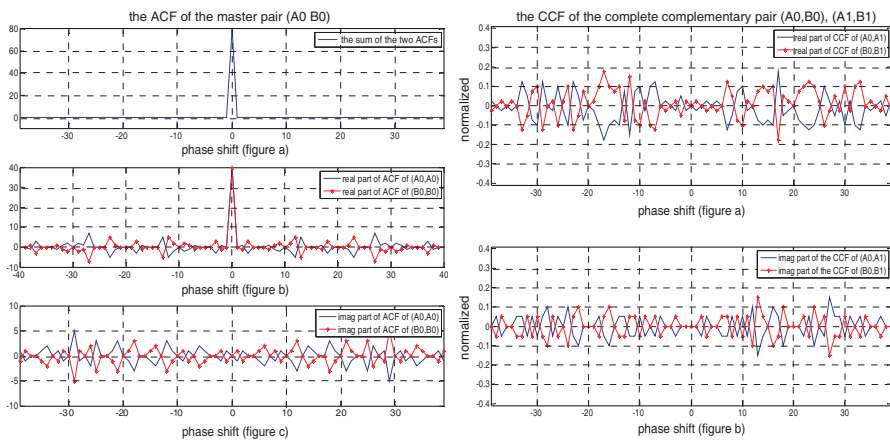


Figure 5. Correlation Performance of CC-S.

Table 2. Imaging qualities of point targets of CC-S case.

Targets	Azimuth (m)	Range (m)	PSLR (dB)		ISLR/dB	
			Azimuth	Range	Azimuth	Range
Target 1	0.889	3.33	-13.36	-34.34	-10.20	-24.38
Target 2	0.888	3.34	-13.33	-34.34	-10.21	-24.38
Target 3	0.889	3.33	-13.34	-34.33	-10.23	-24.38

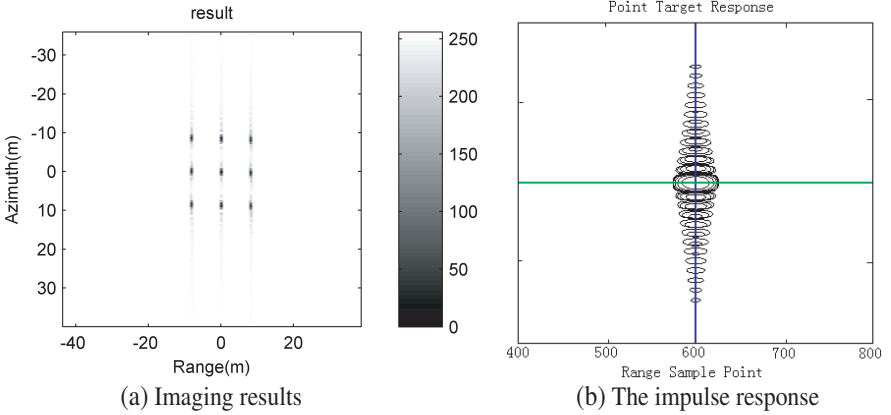
**Figure 6.** Ideal impulse response of point targets.

Figure 5 lists the correlation property of the CC-S $\{(A_0, B_0), (A_1, B_1)\}$ and shows the perfect range dimension compression property. According to the imaging algorithm described in Section 3, we can get the imaging results described in Fig. 6.

We select three point targets to analyze the imaging qualities. The simulation and analytical results validate the imaging algorithm. Fig. 6(b) indicates that the MIMO SAR system based on CC-S satisfies ideal range pulse compression. Fig. 7 shows that the range impulse response of CC-S and LFM. The range PSLR and ISLR are -34.337 dB and -24.375 dB for the CC-S case respectively, and -13.292 dB and -10.411 dB for traditional LFM case. For imaging results, the MIMO SAR system based on CC-S keeps the original theoretic resolution and the co-channel interference is canceled. The phenomena can be interpreted as the contribution of complete orthogonality of CC-S.

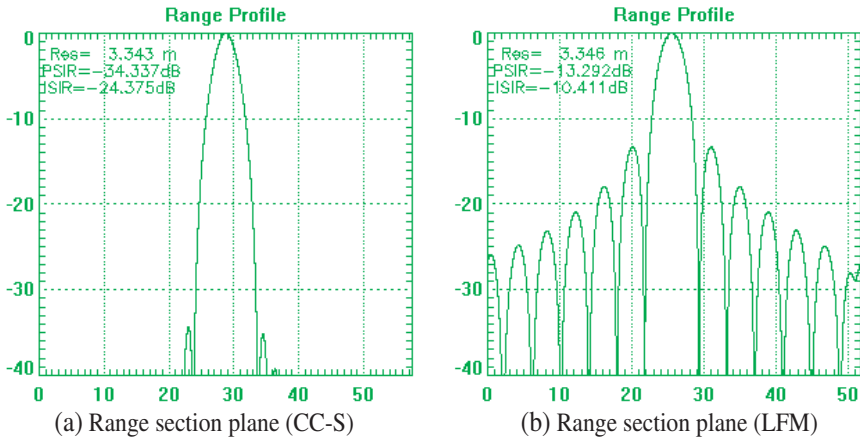


Figure 7. Range impulse response of CC-S and LFM.

5. CONCLUSION

This paper establishes the transmitter model of MIMO SAR based on CC-S and proposes corresponding matched filter. Unlike traditional SAR system which employs LFM, the MIMO SAR system based on CC-S can depress the sidelobe perfectly and further improve the PSIR and ISLR under the condition that the resolution keeps the ideal value. The above property enhances the interference capability. This paper only discusses the application of CC-S in MIMO SAR system. Given that the new system is in infancy, there are still some problems which should be resolved urgently:

- 1) How to increase the bandwidth considering the practical hardware and the limit of the Doppler. The above problem mainly restricts the development of the high resolution imaging and GMTI.
- 2) How to investigate merit and flaw of different imaging algorithms employing CC-S. Solving this problem will be helpful for the whole design of MIMO SAR system.

ACKNOWLEDGMENT

This work was supported by the Program for New Century Excellent Talents in University, Ministry of Education, China (Grant No. NCET-06-0166).

REFERENCES

1. Rabideau, D. J. and P. Parker, "Ubiquitous MIMO multifunction digital array radar," *Conference Record of the 37th Asilomar Conference on Signal, Systems and Computers*, 1057–1064, 2003.
2. Fishler, E., A. Haimovich, R. Blum, et al., "MIMO radar: An idea whose time has come," *Proceedings of the IEEE Conference on Radar*, 71–78, 2004.
3. Yang, Y. and R. S. Blum, "Minimax robust MIMO radar waveform design," *IEEE Journal of Selected Topics in Signal Processing*, Vol. 1, No. 1, 147–155, 2007.
4. De Maio, A. and M. Lops, "Design principles of MIMO radar detectors," *IEEE Transaction on Aerospace and Electronic Systems*, Vol. 43, No. 3, 886–898, 2007.
5. Du, C., J. S. Thompson, and Y. Petillot, "Predicted detection performance of MIMO radar," *IEEE Signal Processing Letters*, Vol. 15, 83–86, 2008.
6. Li, N., J. Tang, and Y. N. Peng, "Adaptive pulse compression of MIMO radar based on GSC," *Electronics Letters*, Vol. 44, No. 20, 2008.
7. Li, J. and P. Stoica, *MIMO Radar Signal Processing*, Wiley-IEEE Press, 2008.
8. Xu, L. Z. and J. Li, "Iterative generalized-likelihood ratio test for MIMO radar," *IEEE Transaction on Signal Processing*, Vol. 55, No. 6, 2375–2385, 2007.
9. Li, J. and P. Stoica, "MIMO radar with collocated antennas," *IEEE Signal Processing Magazine*, Vol. 24, No. 5, 106–114, 2007.
10. Bekkerman, I. and J. Tabrikian, "Target detection and localization using MIMO radars and sonars," *IEEE Transactions on Signal Processing*, Vol. 54, No. 10, 3873–3883, 2006.
11. Xu, L. Z. and J. Li, "Adaptive techniques for MIMO radar," *The 4th IEEE Workshop Sensor Array Multi-Channel Processing*, 258–262, 2006.
12. Bekkerman, I. and J. Tabrikian, "Spatially coded signal model for active arrays," *IEEE International Conference on Acoustics Speech, and Signal Processing, Proceedings (II)*, 209–212, 2004.
13. Zhao, G. H, B. X. Chen, and S. P. Zhu, "Direction synthesis in DOA estimation for monostatic multiple input output (MIMO) radar based on synthetic impulse and aperture radar (SIAR) and its performance analysis," *Science in China Series E: Technological Sciences*, Vol. 51, No. 6, 656–673, 2008.

14. Jin, M., G. S. Liao, and J. Li, "Joint DOD and DOA estimation for bistatic MIMO radar," *Signal Process*, Vol. 89, 244–251, 2009.
15. Li, J., P. Stoica, L. Z. Xu, and W. Roberts, "On parameter identifiability of MIMO radar," *IEEE Signal Processing Letters*, 968–971, Vol. 14, No. 12, 2007.
16. Tang, J., N. Li, Y. Wu, and Y. N. Peng, "On detection performance of MIMO radar: A relative entropy-based study," *IEEE Signal Processing Letters*, Vol. 16, No. 3, 2009.
17. Haimovich, A. M., R. S. Blum, and L. J. Cimini, "MIMO radar with widely separated antennas," *IEEE Signal Processing Magazine*, Vol. 25, No. 1, 116–129, 2008.
18. Fishler, E., A. M. Haimovich, R. S. Blum, et al., "Spatial diversity in radars-models and detection performance," *IEEE Transactions on Signal Processing*, Vol. 54, No. 3, 823–838, 2006.
19. Lehmann, N. H., E. Fishler, A. M. Haimovich, et al., "Evaluation of transmit diversity in MIMO-radar direction finding," *IEEE Transactions on Signal Processing*, Vol. 55, No. 5, 2215–2225, 2007.
20. Deng, H., "Polyphase code design for orthogonal netted radar systems," *IEEE Transaction on Signal Processing*, Vol. 52, No. 11, 3126–3135, 2004.
21. Yang, M. L., S. H. Zhang, B. X. Chen, and H. Y. Zhang, "A novel signal approach for the multi-carrier MIMO radar," *Journal of Electronics and Information Technology*, Vol. 31, No. 1, 147–151, 2009.
22. Liu, B., C. L. Han, and J. H. Miao, OFD-LFM signal design and performance analysis for MIMO radar," *Journal of University of Electronics Science and Technology of China*, Vol. 38, No. 1, 28–31, 2009.
23. Stoica, P., J. Li, and Y. Xie, "On probing signal design for MIMO radar," *IEEE Transactions on Signal Processing*, Vol. 55, No. 8, 4151–4161, 2007.
24. Duan, N. J., D. W. Wang, and X. Y. Ma, "Approach of wave-number domain imaging for the MIMO radar system with small-squint angle," *Journal of Air Force Radar Academy*, Vol. 22, No. 3, 169–172, 2008.
25. Wang, H. J., Y. Su, Y. T. Zhu, and H. B. Xu, "MIMO radar imaging based on spatial spectral-domain filling," *Acta Electronica Sinica*, Vol. 36, No. 6, 1242–1246, 2009.
26. Li, J., X. Y. Zhang, and P. Stoica, "MIMO SAR imaging: Signal synthesis and receiver design," *The 2th IEEE International*

- Workshop on Imaging Computational Advance in Multi-Sensor Adaptive Processing*, 89–92, 2007.
27. Sun, J. P, S. Y. Mao, G. H. Wang, and W. Hong, “Extended exact transfer function algorithm for bistatic SAR of translational invariant case,” *Progress In Electromagnetics Research*, PIER 99, 89–108, 2009.
 28. Li, S. F., J. Chen, L. Q. Zhang, and Y. Q. Zhou, “Construction of quadri-phase complete complementary pairs applied in MIMO radar systems,” *The 9th International Conference on Signal Processing*, 2298–2301, 2008.